

PSEUDO- AND QUASI-PDFs IN THE BFKL APPROXIMATION*

GIOVANNI ANTONIO CHIRILLI

Institut für Theoretische Physik, Universität Regensburg
Universitätsstrasse 31, 93040 Regensburg, Germany

*Received 1 December 2022, accepted 13 December 2022,
published online 25 May 2023*

I will present the formalism one may use to study the behavior of the Ioffe-time distribution at large distances and show that the pseudo-PDF and quasi-PDF are very different in this regime. Using light-ray operators, I will also show that the higher twist corrections of the quasi-PDF come in not as inverse powers of P but as inverse powers of $x_B P$.

DOI:10.5506/APhysPolBSupp.16.5-A29

1. Introduction

The Euclidean formulation of the lattice gauge theory does not allow for direct calculations of the PDFs. So far, the most successful procedure to overcome this difficulty is given by the study of equal-time correlators in coordinate space called the Ioffe-time distributions. Two different Fourier transforms of the Ioffe-time distributions lead to the quasi-PDF [1] and the pseudo-PDF [2].

For the first time, in Ref. [3], we obtained the behavior of the gluon Ioffe-time distribution at large longitudinal distances as well as the low- x_B behavior of the quasi-PDF and pseudo-PDF. Using the light-ray operators, obtained as an analytic continuation of local twist-two operators [5, 6], we extracted also the leading twist (LT) and next-to-leading twist (NLT) contributions.

2. Pseudo-PDF and quasi-PDF from Ioffe-time distribution

The pseudo-PDF and quasi-PDF are obtained from two different Fourier transforms of the Ioffe-time distributions. As we will see, these differences

* Presented at the Diffraction and Low- x 2022 Workshop, Corigliano Calabro, Italy, 24–30 September, 2022.

will lead to two completely different behaviors at small- x_B . The gluon bilocal operator, $M_{\mu\alpha;\lambda\beta} \equiv \langle P|G_{\mu\alpha}(z)[z,0]G_{\lambda\beta}(0)|P\rangle$, defining the Ioffe-time distribution, can be decomposed in terms of six tensor structures proportional to invariant amplitudes of the type $\mathcal{M}(z^2, P^2)$, using the proton momentum P^μ , the coordinate z^μ , and the metric tensor $g^{\mu\nu}$. The light-cone gluon distribution is determined from $g_\perp^{\alpha\beta} M_{+\alpha;+\beta}(z^+, P)$ with z taken on the light-cone and proportional to the invariant amplitude

$$g_\perp^{\alpha\beta} M_{+\alpha;+\beta}(z^+, P) = 2(P^-)^2 \mathcal{M}_{pp}(z \cdot p, 0). \quad (1)$$

As usual, we define the light-cone coordinates $x^\pm = \frac{x^0 \pm x^3}{\sqrt{2}}$, and light-cone vectors n^μ and n'^μ such that $n \cdot n' = 1$, $n \cdot x = x^-$, and $n' \cdot x = x^+$.

The relation between the gluon PDF $D_g(x_B)$ and the amplitude \mathcal{M}_{pp} is given by

$$\mathcal{M}_{pp}(z \cdot P, 0) = \frac{1}{2} \int_{-1}^1 dx_B e^{iz \cdot P x_B} x_B D_g(x_B). \quad (2)$$

The gluon Ioffe-time distribution $\mathcal{M}_{pp}(z \cdot P, z^2)$, with $z \cdot P$ the Ioffe-time parameter, is given in terms of the zeroth and transverse components as (subscript pp indicates projection along the proton momentum P^μ)

$$M_{0i;i0} + M_{ji;ij} = 2P_0^2 \mathcal{M}_{pp}. \quad (3)$$

Since in the high-energy (Regge) limit the transverse components are suppressed, while the 0th and 3rd components cannot be distinguished, calculating the behavior of the left-hand side (LHS) of (1) will be equivalent, at high-energy, to calculating the behavior of RHS of (3). The momentum-density pseudo-PDF is defined as the Fourier transform with respect to $z \cdot P$, *i.e.* a Fourier transform with respect to P keeping its orientation fixed. Thus, we define the gluon pseudo-PDF as

$$G_p(x_B, z^2) = \int \frac{d\varrho}{2\pi} e^{-i\varrho x_B} \mathcal{M}_{pp}(\varrho, z^2), \quad (4)$$

where we defined $\varrho \equiv z \cdot P$, and the subscript p stands for pseudo. The momentum-density quasi-PDF is defined, instead, as the Fourier transform with respect to z^μ keeping its orientation fixed. Let us define the vector $\xi^\mu = \frac{z^\mu}{|z|}$, and $P_\xi = P \cdot \xi$. The quasi-PDF is then defined as

$$G_q(x_B, P_\xi) = P_\xi \int \frac{d\varsigma}{2\pi} e^{-i\varsigma P_\xi x_B} \mathcal{M}_{pp}(\varsigma P_\xi, \varsigma^2), \quad (5)$$

where the subscript q stands for quasi. We will calculate the large distance (large ϱ) behavior of the Ioffe-time distribution $\mathcal{M}_{pp}(\varrho, z^2)$, and the low- x_B behavior of the gluon pseudo-PDF (4), and of the gluon quasi-PDF (5).

3. Low- x_B behavior from high-energy OPE

To get the low- x_B behavior of the gluon pseudo- and quasi-PDF we should first consider the behavior of the Ioffe-time distribution for large values of the ϱ parameter using the high-energy operator product expansion (HE-OPE) (see [7] for review).

The HE-OPE procedure requires that one calculates the coefficient function (Impact Factor) first, and then the resummation of the relevant logarithms is obtained through the evolution with respect to the rapidity parameter of the resulting operators. The aforementioned procedure in the saddle point approximation is [3]

$$\mathcal{M}_{pp}(\varrho, z^2) \simeq \frac{3N_c^2}{128} \frac{Q_s \sigma_0}{\varrho |z|\eta^{1/2}} \left(\frac{2\varrho^2}{z^2 M_N^2} + i\epsilon \right)^{\bar{\alpha}_s 2 \ln^2} e^{-\frac{1}{\eta} \ln^2 \frac{Q_s |z|}{2}}, \quad (6)$$

where we defined $\eta \equiv 7\zeta(3)\bar{\alpha}_s \ln(2\varrho^2/(z^2 M_N^2) + i\epsilon)$, $\bar{\alpha}_s = \frac{\alpha N_c}{\pi}$ and Q_s is the saturation scale, as the subscript indicates, from the Golec-Biernat–Wüsthoff [8] model used. In Eq. (6) (plotted in Fig. 1), the first thing we should notice is that the logarithms resummed by BFKL are $\bar{\alpha}_s \ln\left(\frac{\sqrt{2}\varrho}{|z|M_M}\right)$. The second is that the Ioffe-time ϱ acts like a rapidity parameter. We evolve the distribution in ϱ as long as $\bar{\alpha}_s \ln\left(\frac{\sqrt{2}\varrho}{|z|M_M}\right)$ is of the order of 1, *i.e.* we start the evolution at large values of ϱ and end at smaller ones. The dipole at the smallest value of ϱ is evaluated in the GBW model [8].

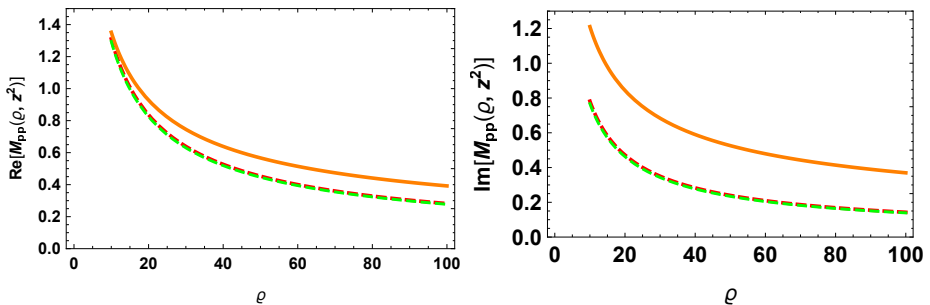


Fig. 1. In the left panel, the orange curve is the numerical evaluation of the real part of Eq. (6), the green dashed curve is the real part of the LT term only, while the red dashed one is the real part of the LT+NLT of Eq. (7). In the right panel we plot the imaginary parts.

Considering the case $0 < \frac{Q_s^2 |z|^2}{4} < 1$, which corresponds to the typical DIS region, taking the first two leading residues, we obtain the twist expansion as [3]

$$\mathcal{M}_{pp}(\varrho, z^2) = \frac{N_c^2}{8\pi^2\bar{\alpha}_s} \frac{Q_s^2\sigma_0}{\varrho} \left(\frac{4\bar{\alpha}_s \left| \ln \frac{Q_s|z|}{2} \right|}{\ln\left(\frac{2\varrho^2}{z^2 M_N^2} + i\epsilon\right)} \right)^{\frac{1}{2}} I_1(\tilde{t}) \left(1 + \frac{Q_s^2|z|^2}{5} \right), \quad (7)$$

$$\text{with } \tilde{t} = \left[4\bar{\alpha}_s \left| \ln \frac{Q_s|z|}{2} \right| \ln\left(\frac{2\varrho^2}{z^2 M_N^2} + i\epsilon\right) \right]^{\frac{1}{2}}.$$

3.1. Gluon pseudo- and quasi-PDF with BFKL resummation

The pseudo-PDF is obtained from Eq. (4) performing the Fourier transform with respect to ϱ . In the saddle point approximation, the result is

$$G_P(x_B, z^2) \simeq -i \frac{3N_c^2}{128\pi} \frac{Q_s\sigma_0}{|z|} \frac{\Gamma(\bar{\alpha}_s 4 \ln 2) \sin\left(\frac{\pi}{2}\bar{\alpha}_s 4 \ln 2\right)}{\sqrt{7\zeta(3)\bar{\alpha}_s \ln\left(\frac{2}{x_B^2 z^2 M_N^2} + i\epsilon\right)}} \text{sign}(x_B) \\ \times \exp\left\{ \frac{-\ln^2 \frac{Q_s|z|}{2}}{7\zeta(3)\bar{\alpha}_s \ln\left(\frac{2}{x_B^2 z^2 M_N^2} + i\epsilon\right)} \right\} \left(\frac{2}{x_B^2 z^2 M_N^2} + i\epsilon \right)^{\bar{\alpha}_s 2 \ln 2}. \quad (8)$$

In result (8) one can immediately observe the typical low- x_B resummation of logarithms $\bar{\alpha}_s \ln 1/x_B$ with $\bar{\alpha}_s 2 \ln 2$ the famous Pomeron intercept. Similarly, we can perform the Fourier transform (4) in the leading and next-to-leading twist approximation:

$$G_P(x_B, z^2) = \frac{N_c^2 Q_s^2 \sigma_0}{16\pi^3 \bar{\alpha}_s} \left(1 + \frac{Q_s^2 |z|^2}{5} \right) I_0(h) + O\left(\frac{Q_s^4 |z|^4}{16}\right), \quad (9)$$

with $h = \left[2\bar{\alpha}_s \left| \ln 4 / (|z|^2 Q_s^2) \right| \ln 2 / (x_B^2 |z^2| M_N^2) \right]^{\frac{1}{2}}$, and I_0 the modified Bessel function. In Fig. 2, we plot the gluon pseudo-PDF with the BFKL resummation Eq. (8) (orange curve), and the LT term and the LT plus NLT (green dashed and red dashed curves respectively). We observe that the BFKL resummation result agrees with the LT and LT+NLT result in the region of moderate x_B . When we move into the low- x_B region, we notice a strong disagreement which confirms the necessity of a $\ln \frac{1}{x_B}$ resummation represented by the BFKL equation.

For the quasi-PDF case, we need to perform a Fourier transform with respect to a different parameter. Let us introduce the real parameter ς such that $-z^2 = \varsigma^2 > 0$, and the four-vector $\xi^\mu \equiv \frac{z^\mu}{|z|} = \frac{z^\mu}{|\varsigma|}$ with $|z| = \sqrt{-z^2}$. The quasi-PDF are defined as the Fourier transform of the coordinate-space gluon distributions keeping, this time, the orientation of the vector z^μ fixed. Thus, using the definition of the gluon quasi-PDF Eq. (5), performing the

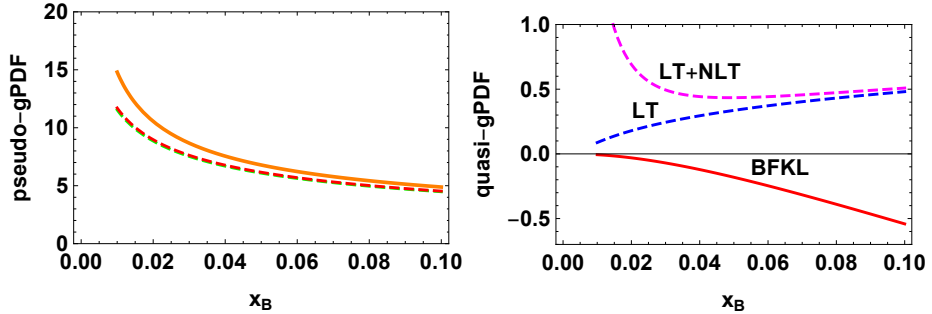


Fig. 2. In the left panel, we plot the pseudo-PDF with BFKL resummation (orange curve), and the LT (green dashed curve) and LT+NLT (red dashed curve) of the pseudo-PDF result. In the right panel, we plot quasi-PDF with BFKL resummation (real part), the LT and LT+NLT (real part). The curves are plotted in the range $x_B \in [0.01, 0.1]$ with $P_\xi = 4$ GeV. The value of x_B is between 0.1 to 0.01 in both plots.

integration over ς (recall that we are using $\gamma = \frac{1}{2} + i\nu$) and then taking the saddle point approximation for the last integration over ν , we get

$$G_q(x_B, P_\xi) \simeq \frac{-3N_c^2 Q_s \sigma_0}{256(P_\xi |x_B|)^{-1}} \left(-\frac{2P_\xi^2}{M_N^2} + i\epsilon \right)^{\bar{\alpha}_s 2 \ln 2} \frac{1}{\sqrt{\chi}} e^{-\frac{1}{\chi} \ln^2 \frac{Q_s}{2P_\xi |x_B|}}. \quad (10)$$

where we defined $\chi \equiv 7\zeta(3)\bar{\alpha}_s \ln \left(-\frac{2P_\xi^2}{M_N^2} + i\epsilon \right)$. We notice that, in the gluon quasi-PDF case, the usual exponentiation of the Pomeron intercept (the LO BFKL eigenvalues $\aleph(\gamma)$), which indicates the resummation of large logarithms of $\frac{1}{x_B}$, is absent.

The result for the leading and next-to-leading twist gluon quasi-PDF is

$$G_q(x_B, P_\xi) = -\frac{N_c^2 Q_s^2 \sigma_0}{16\bar{\alpha}_s^2 \pi^3} \frac{1}{2\pi i} \int_{1-i\infty}^{1+i\infty} d\omega \omega \left(-\frac{2P_\xi^2}{M_N^2} + i\epsilon \right)^{\frac{2}{\omega}} \times \left(-\frac{4P_\xi^2 x_B^2}{Q_s^2} + i\epsilon \right)^{\frac{\bar{\alpha}_s}{\omega}} \left(1 + \frac{2\bar{\alpha}_s Q_s^2}{5\omega P_\xi^2 x_B^2} \right). \quad (11)$$

What one should notice in result (11) is the strong enhancement of the NLT term with respect to the LT term due to the $\frac{1}{P_\xi^2 x_B^2}$ factor which increases as x_B decreases.

4. Conclusions

We may conclude that the pseudo-PDF and the quasi-PDF have very different behavior at low- x_B . The physical origin of the difference between the two distributions is due to the two different Fourier transforms under which they are defined. Indeed, in the pseudo-PDF case, the scale is the resolution, *i.e.* the square of the length of the gauge link separating the bi-local operator. On the other hand, in the quasi-PDF case, the scale is the energy, *i.e.* the momentum of the hadronic target (the nucleon) projected along the direction of the gauge link. Therefore, if on one hand, the pseudo-PDF has the typical behavior of the gluon distribution at low- x_B , on the other hand, the quasi-PDF has a rather unusual low- x_B behavior (see figure 2).

REFERENCES

- [1] X. Ji, *Phys. Rev. Lett.* **110**, 262002 (2013), [arXiv:1305.1539 \[hep-ph\]](#).
- [2] A.V. Radyushkin, *Phys. Rev. D* **96**, 034025 (2017), [arXiv:1705.01488 \[hep-ph\]](#).
- [3] G.A. Chirilli, *J. High Energy Phys.* **2022**, 064 (2022), [arXiv:2111.12709 \[hep-ph\]](#).
- [4] I. Balitsky, *Int. J. Mod. Phys.: Conf. Ser.* **25**, 1460024 (2014).
- [5] I. Balitsky, V. Kazakov, E. Sobko, [arXiv:1310.3752 \[hep-th\]](#).
- [6] I. Balitsky, *J. High Energy Phys.* **2019**, 042 (2019), [arXiv:1812.07044 \[hep-th\]](#).
- [7] I. Balitsky, in: M. Shifman (Ed.) «At The Frontier of Particle Physics», *World Scientific*, Singapore 2001, pp. 1237–1342, [arXiv:hep-ph/0101042](#).
- [8] K.J. Golec-Biernat, M. Wusthoff, *Phys. Rev. D* **59**, 014017 (1998), [arXiv:hep-ph/9807513](#).